

# SEARCH FOR GAMMA-RAY EMISSION FROM FOUR ACCRETING MILLISECOND PULSARS WITH *FERMI*/LAT

YI XING AND ZHONGXIANG WANG

Shanghai Astronomical Observatory, Chinese Academy of Sciences,  
 80 Nandan Road, Shanghai 200030, China

*Draft version November 29, 2012*

## ABSTRACT

We report our search for  $\gamma$ -ray emission in the energy range from 100 MeV to 300 GeV from four Accreting Millisecond Pulsars (AMPs), SAX J1808.4–3658, IGR J00291+5934, XTE J1814–338, and XTE J0929–314. The data are from four-year observations carried out by Large Area Telescope (LAT) onboard the *Fermi*  $\gamma$ -ray Space Telescope. The AMPs were not detected, and their  $\gamma$ -ray luminosity upper limits we obtain are  $5.1 \times 10^{33}$  ergs s<sup>−1</sup> for SAX J1808.4–3658,  $2.1 \times 10^{33}$  ergs s<sup>−1</sup> for IGR J00291+5934,  $1.2 \times 10^{34}$  ergs s<sup>−1</sup> for XTE J1814–338, and  $2.2 \times 10^{33}$  ergs s<sup>−1</sup> for XTE J0929–314. We compare our results with  $\gamma$ -ray irradiation luminosities required for producing optical modulations seen from the companions in the AMPs, which has been suggested by Takata et al. (2012), and our upper limits have excluded  $\gamma$ -ray emission as the heating source in these systems except XTE J0929–314, the upper limit of which is not deep enough. Our results also do not support the model proposed by Takata et al. (2012) that relatively strong  $\gamma$ -ray emission could arise from the outer gap of a high-mass neutron star controlled by the photon-photon pair-creation for the AMPs. Two AMPs, SAX J1808.4–3658 and IGR J00291+5934, have the measurements of their spin-down rates, and we derive the upper limits of their  $\gamma$ -ray conversion efficiencies, which are 57% and 3%, respectively. We discuss the implications to the AMP systems by comparing the efficiency upper limit values with that of 20  $\gamma$ -ray millisecond pulsars (MSP) detected by *Fermi* and the newly discovered transitional MSP binary J1023+0038.

*Subject headings:* pulsars: general – stars: neutron – binaries: close – gamma rays: stars

## 1. INTRODUCTION

Accreting millisecond pulsars (AMPs) are all in low mass X-ray binary (LMXB) systems, spinning at frequencies more than 100 Hz and containing companion stars with masses less than  $1 M_{\odot}$  (Patruno & Watts 2012). The periodical pulsed emission from AMPs is accretion powered, which distinguishes them from normal radio millisecond pulsars (MSPs) that are powered by rotation. AMPs are believed to be the progenitors of MSPs spun up from old slowly rotating neutron stars (NSs) by the recycling scenario (Alpar et al. 1982; Bhattacharya & van den Heuvel 1991; Srinivasan 2010), that is when a NS in a binary system switches off the pulsed radio emission, the mass and angular momentum of the companion star are transferred to the NS through accretion, producing a recycled pulsar that eventually spins at a period of milliseconds. The currently known AMPs are all transient systems with recurrent times of years. Evolution of their accretion disks leads to weeks-long outbursts, during which pulsed X-ray emission is detected.

The first known AMP SAX J1808.4–3658 was found by the *BeppoSAX* mission in 1996 (in 't Zand et al. 1998) and discovered to have pulsed X-ray emission with the *Rossi X-ray Timing Explorer* (RXTE) during its 1998 outburst (Wijnands & van der Klis 1998; Chakrabarty & Morgan 1998). Since then, over a dozen of AMP systems have been discovered (Patruno & Watts 2012). One interesting property of AMP binaries was first pointed out by Burderi et al. (2003): because the orbital optical modulation seen in SAX J1808.4–3658

has a larger than expected amplitude in the quiescent state (Homer et al. 2001), the AMP probably switches to be rotation-powered and thus is able to provide the required energy output to heating of the companion. Followup observations of SAX J1808.4–3658 at X-ray and optical energies have firmly verified the inconsistency between the large optical modulation and low X-ray luminosity in quiescence (Campana et al. 2004; Deloye et al. 2008; Wang et al. 2009b). X-ray emission from accreting compact stars normally is the heating source to cause orbital optical modulations seen in LMXBs (e.g., van Paradijs & McClintock 1995). In addition, the inconsistency has also been seen in two other AMP systems, IGR J00291+5934 and XTE J1814–338 (D'Avanzo et al. 2007; Jonker et al. 2008; D'Avanzo et al. 2009), which suggests a common property of being able to switch to be radio pulsars in quiescence for AMP systems, although no direct evidence has been found from radio observations of them (Burgay et al. 2003).

The more recent discovery of the millisecond pulsar binary PSR J1023+0038 (Archibald et al. 2009) has strengthened the likelihood of the radio-pulsar switching property of the AMP systems. The binary is considered to be the first system found at the end of its evolution from a LMXB to a MSP binary, as a short-term accretion disk was seen in it (Wang et al. 2009a, 2012).  $\gamma$ -ray emission from PSR J1023+0038 was also found from observations carried out by *Fermi* Gamma-ray Space Telescope (Tam et al. 2010). Considering PSR J1023+0038 as an end product of LMXB evolution closely related to AMP systems, Takata et al. (2012) studied possible  $\gamma$ -

ray emission mechanisms for the AMP systems known with large-amplitude optical modulations (see Table 1). In their work, they attributed the optical modulations of the AMP systems to  $\gamma$ -ray irradiation of the companions, which required  $\gamma$ -ray luminosity  $L_\gamma > 10^{32} - 10^{34}$  ergs  $s^{-1}$ . The predicted  $\gamma$ -ray emission is possibly detectable by *Fermi*, and any detection would provide strong evidence for the existence of radio pulsars in these AMP systems in quiescence. We thus searched for  $\gamma$ -ray emission from the four AMPs in the data obtained by *Fermi* and report our results in this paper. The general properties of the four AMPs are summarized in Table 1.

In § 2 we describe the data from the *Fermi* Large Area Telescope (LAT) observations and our analysis of the data for the four AMPs. We provide the results in § 3 and discuss the implications of our results in § 4.

## 2. OBSERVATION AND DATA ANALYSIS

LAT is an imaging instrument onboard the *Fermi* Gamma-ray Space Telescope. Its main objective is to conduct continuous  $\gamma$ -ray monitoring of a large sample of sources in energy range from 20 MeV to 300 GeV with much improved sensitivity compared with former  $\gamma$ -ray telescopes (Atwood et al. 2009). In our data analysis we selected LAT events within 15 degrees centered at the positions of the four AMPs during time period from the start of the releasing of *Fermi* public data 2008-08-04 15:43:36 (UTC) to 2012-07-08 18:59:57 (UTC) from the *Fermi* Pass 7 database. We included events in an energy range from 100 MeV to 300 GeV. Following recommendations of the LAT team, we required events zenith angle to be less than 100 degrees to prevent the Earth's limb contamination, and excluded events in time intervals when spacecraft events affected the quality of the LAT data.

### 2.1. Maximum likelihood analysis

We rejected events below 200 MeV and included only events in energy range from 200 MeV to 300 GeV for the likelihood analysis, because the instrument response function of LAT has relative large uncertainties in lower energy range. We included all sources within 20 degrees centered at the four AMPs to make the source models based on the *Fermi* 2-year catalog. Most of them are point sources, while a few of them are diffuse sources. The spectral function forms of these sources were selected the same as those in the catalog. We let the spectral normalization parameters of sources within 3 degrees from the four AMPs free, and fixed all the other parameters of sources included in our source models to their catalog values. The four AMPs we are interested in were not included in the *Fermi* catalog. We modeled the  $\gamma$ -ray spectra of them with a exponentially cut-off power law which is the typical spectral form of pulsars (Abdo et al. 2009, 2010c). The exponentially cut-off power law can be expressed by  $dN/dE = N_0 E^{-\Gamma} \exp[-(E/E_{cut})]$ , where  $\Gamma$  is the spectral index and  $E_{cut}$  is the cut-off energy. In addition we considered the galactic and extragalactic diffuse emission using the model gal2yearp7v6.v0.fits and the spectrum file iso\_p7v6source.txt, respectively. The value of the galactic diffuse emission model and the normalization of the extragalactic diffuse emission model were let free.

We performed standard binned likelihood analysis with the LAT science tools software package v9r27p1. The

binned likelihood used events in a square region instead of a circle, so we selected events inside a  $20^\circ \times 20^\circ$  region centered at each interested source, which is nearly the inscribed square of the circular region we selected above. We obtained the Test Statistic (TS) of the four AMPs and found IGR J00291+5934, XTE J1814-338, and XTE J0929-314 have TS of  $\sim 0$ , and SAX J1808.4-3658 has TS of  $\sim 3$ . The TS value is approximately the square of the detection significance of a source and it can be used to assess whether a source exists or not. Actually in the *Fermi* source catalog only sources with TS greater than 25 were included, which corresponds to the detection significance of  $4.6\sigma$  (Abdo et al. 2010b). The TS values of the four AMPs thus indicate that they were not detected by *Fermi*/LAT in 200 MeV – 300 GeV band.

### 2.2. Flux Upper limit Calculation

The  $\gamma$ -ray flux upper limits of these four AMPs were estimated by the binned likelihood analysis with the source models we described above. We fixed the  $\Gamma$  and  $E_{cut}$  parameters of the spectral models of the four AMPs to 1.4 and 1.6 GeV respectively, which are the averaged spectral parameters of the eight MSPs *Fermi* detected during the first six months monitoring (Abdo et al. 2009, 2010c) and derived from the *Fermi* 2-year catalog (see Table 2). The spectral normalization factors were let free. We extracted the upper limits of normalization factors by increasing these factors until the maximum likelihood values decreased by  $e/2$  in logarithm, following the procedure introduced by the LAT team. Then using the upper limits of normalization factors we derived the 95% flux upper limits in energy range from 100 MeV to 300 GeV by integrating the spectral models. Assuming isotropic  $\gamma$ -ray emission, the upper limits of the  $\gamma$ -ray luminosities of these four sources were calculated, where the distance values of the sources listed in Table 1 were used.

### 2.3. Timing analysis

We performed timing analysis of the *Fermi*/LAT observations of the four AMPs to search for any  $\gamma$ -ray pulsations. We included events in energy range from 100 MeV to 300 GeV within 1 degree centered at the positions of these four sources, and folded them into 20 phase bins using X-ray ephemerides (Table 1). We obtained the folded light curves of these sources (Figure 1) and made  $\chi^2$  test to identify possible presence of  $\gamma$ -ray pulsations. The  $\chi^2$  values of the four folded light curves are in the range of 11–28, which are comparable to the 19 degrees of freedom and thereby indicate no significant  $\gamma$ -ray pulsations were detected (Larsson 1996). In addition for SAX J1808.4-3658 and IGR J00291+5934, which had X-ray outbursts after August 2008 under the *Fermi* coverage, we searched their  $\gamma$ -ray pulsations during the outbursts. SAX J1808.4-3658 had the X-ray outbursts in 2008 starting at MJD 54730 with  $\nu$  of 400.97521009 Hz and  $\dot{\nu}$  of  $0.6 \times 10^{-13}$  Hz  $s^{-1}$  (Hartman et al. 2009), and in 2011 starting at MJD 55865 with  $\nu$  of 400.97520981 Hz and non-significant  $\dot{\nu}$  of  $< 4 \times 10^{-13}$  Hz  $s^{-1}$  (Patruno et al. 2012). IGR J00291+5934 had two X-ray outbursts in 2008, one was in MJD 54691.94–54696.77 with  $\nu$  of 598.89213061 Hz and  $\dot{\nu}$  of  $12.3 \times 10^{-13}$  Hz  $s^{-1}$ , and the other was in

MJD 54730.51–54742.89 with  $\nu$  of 598.89213046 Hz and  $\dot{\nu}$  of  $5.7 \times 10^{-13}$  Hz s $^{-1}$  (Patruno 2010). We searched  $\gamma$ -ray pulsations of SAX J1808.4–3658 during MJD 54735–54760 and MJD 55870–55886, and of IGR J00291+5934 during its two outbursts, using their spin parameters given above. No detections of  $\gamma$ -ray pulsations were found from these two sources.

### 3. RESULTS

We found that the four AMPs included in our work were not detected by *Fermi*/LAT at  $\gamma$ -ray energies. We obtained upper limits of their  $\gamma$ -ray luminosities, that are  $5.1d_{3.5}^2 \times 10^{33}$  ergs s $^{-1}$  for SAX J1808.4–3658,  $2.1d_5^2 \times 10^{33}$  ergs s $^{-1}$  for IGR J00291+5934,  $1.2d_8^2 \times 10^{34}$  ergs s $^{-1}$  for XTE J1814–338, and  $2.2d_6^2 \times 10^{33}$  ergs s $^{-1}$  for XTE J0929–314, where  $d$  is the source distance with its subscript indicating the value (in units of kpc; Table 1) used. These results are summarized in Table 1. Two AMPs—SAX J1808.4–3658 and IGR J00291+5934—have measurements of their spin-down rates (Table 1), through which we estimated the spin-down luminosities by  $\dot{E} = 4\pi^2 I \nu \dot{\nu}$ , where  $I$  is the NS moment of inertia and assumed to have a canonical value of  $I = 10^{45}$  g cm $^2$ . We calculated the upper limit of  $\gamma$ -ray conversion efficiency  $\eta_\gamma = L_\gamma / \dot{E}$  for these two sources with the upper limits of  $\gamma$ -ray luminosities we obtained above. SAX J1808.4–3658 has  $\eta_\gamma$  of  $< 0.57d_{3.5}^2$ , and IGR J00291+5934 has  $\eta_\gamma$  of  $< 0.03d_5^2$ . The latter provides a strong constraint on the  $\gamma$ -ray emission from this source.

### 4. DISCUSSION

We searched  $\gamma$ -ray emission from four AMPs, SAX J1808.4–3658, IGR J00291+5934, XTE J1814–338, and XTE J0929–314 with *Fermi*/LAT observations. The four sources were not detected by *Fermi*/LAT in the 200 MeV to 300 GeV energy range. We obtained the 100 MeV to 300 GeV  $\gamma$ -ray luminosity upper limits of these four sources. In addition for two of them, SAX J1808.4–3658 and IGR J00291+5934, with the measurements of the spin-down rates, we estimated the 100 MeV to 300 GeV  $\gamma$ -ray conversion efficiency upper limits. The obtained values of these sources can be used to compare with model predictions of AMPs and conversion efficiencies of  $\gamma$ -ray MSPs, which provides constraints on their properties including  $\gamma$ -ray emission mechanisms.

Depending on different assumptions, a wide range of  $L_\gamma$  values for the four AMPs have been predicted by Takata et al. (2012). Furthermore they have suggested that optical modulations seen in the AMP binaries could be caused by  $\gamma$ -ray irradiation of the companion stars. The irradiation  $\gamma$ -ray luminosities of these sources required for optical modulations were used to constrain the theoretical emission models. For SAX J1808.4–3658, IGR J00291+5934 and XTE J1814–338, the inferred  $\gamma$ -ray irradiation luminosities of  $> 10^{34}$  ergs s $^{-1}$  favored the outer gap model with a high-mass NS controlled by the photon-photon pair-creation between  $\gamma$ -rays and X-rays from full surface cooling emission, or the outer gap model controlled by the magnetic pair-creation process (Takata et al. 2012). Such a high luminosity can not be produced by the outer gap model controlled by the photon-photon pair-creation between  $\gamma$ -rays and X-rays from the heated polar cap because an unreasonably high

NS magnetic field is required. For XTE J0929–314 with a lower inferred  $\gamma$ -ray irradiation luminosity of  $10^{32}$ – $10^{33}$  ergs s $^{-1}$ , the outer gap model with a low-mass NS controlled by the photon-photon pair-creation between  $\gamma$ -rays and X-rays from full surface cooling emission might be preferred (Takata et al. 2012).

In our work, we found that the  $\gamma$ -ray luminosities of SAX J1808.4–3658 and IGR J00291+5934 observed by *Fermi*/LAT had the upper limits of  $5.1d_{3.5}^2 \times 10^{33}$  ergs s $^{-1}$  and  $2.1d_5^2 \times 10^{33}$  ergs s $^{-1}$  respectively, which are significantly lower than the required  $\gamma$ -ray irradiation luminosities of these two sources. For XTE J1814–338 and XTE J0929–314, the  $\gamma$ -ray luminosity upper limits of  $1.2d_8^2 \times 10^{34}$  ergs s $^{-1}$  and  $2.2d_6^2 \times 10^{33}$  ergs s $^{-1}$  are consistent with the required  $\gamma$ -ray irradiation luminosities. However for XTE J1814–338, the  $\gamma$ -ray irradiation luminosity lower limit given by Takata et al. (2012) is nearly equal to the luminosity upper limit we obtained. Considering the actual luminosities of these AMPs might be significantly smaller than the upper limits, the *Fermi* observations of these sources indicate that the  $\gamma$ -ray emission of three AMPs, SAX J1808.4–3658, IGR J00291+5934, and XTE J1814–338, are lower than the values needed to interpret the optical modulations. Thus  $\gamma$ -ray irradiation from the AMPs should not be the main heating source of their companions. The irradiation from release of the rotational energy of the pulsars should be preferred, which indeed provide the required energy output of  $10^{33}$ – $10^{34}$  ergs s $^{-1}$  to heat the companions (Burderi et al. 2003, Table 1), although there are a few unresolved theoretical uncertainties in this model (Burderi et al. 2003; Takata et al. 2012).

$\gamma$ -ray emission from pulsars is generally agreed to originate from accelerations of charged particles, while it is still uncertain where the accelerations occur. At present there are polar cap, outer gap, and slot gap models to be advanced to interpret the high energy emission of pulsars. The polar cap model (Ruderman & Sutherland 1975) has acceleration regions near the surface of a NS, which predicts pulsed emission aligned with the magnetic poles. The model fails to interpret the  $\gamma$ -ray pulsed profiles of pulsars because most of pulsars have two sharp peaks which are not aligned with radio peaks (Abdo et al. 2009, 2010c). The outer gap (Muslimov & Harding 2004) and slot gap models (Cheng et al. 1986) have acceleration regions along the last open field lines to near the light cylinder, starting from the null surface or polar cap, respectively. The two models both predict to have wide-fan beams which are not aligned with magnetic poles so that they are more preferred to interpret  $\gamma$ -ray emission from pulsars. Comparing with that on the basis of the outer gap model predicted by Takata et al. (2012), our results basically rule out their model of a high-mass NS controlled by the photon-photon pair-creation between  $\gamma$ -rays and X-rays from full surface cooling emission for SAX J1808.4–3658, IGR J00291+5934 and XTE J1814–338. For XTE J0929–314, the outer gap emission with a low-mass NS is predicted and our results is still consistent with their model prediction.

The newly born MSP PSR J1023+0038 from an LMXB system has been detected by *Fermi*/LAT with a detection significance of  $\sim 7\sigma$  in the 200 MeV to 20 GeV band (Tam et al. 2010), which greatly motivated our search

for  $\gamma$ -ray emission from the AMPs to verify the possible existence of rotation-powered pulsars in the quiescent state. However, although many  $\gamma$ -ray MSPs have been detected by *Fermi*/LAT (Abdo et al. 2009, 2010c), no  $\gamma$ -ray AMPs have been found. In our work we gave the upper limits of 100 MeV to 300 GeV  $\eta_\gamma$  for two AMPs, that are 57% for SAX J1808.4–3658 and 3% for IGR J00291+5934. We compared them with MSPs detected by *Fermi*/LAT. In the *Fermi* 2-year catalog there are 38 possible  $\gamma$ -ray MSPs, among which 20 are confirmed MSPs that have typical spectral form of pulsars (exponentially cut-off power law) and pulsations detected in  $\gamma$ -ray band. A summary of these 20 MSPs is given in Table 2. We calculated the 100 MeV to 100 GeV  $\eta_\gamma$  of these MSPs with flux values given in the catalog and timing parameters listed in Table 2. These sources'  $\eta_\gamma$  are plotted in Figure 2, with uncertainties derived from flux uncertainties given in the catalog. In addition the uncertainties related to distance measurements are approximately 60% presuming 30% distance uncertainties. As can be seen, the  $\gamma$ -ray conversion efficiency of  $< 3\%$  of IGR J00291+5934 lies in the very lower range of that of  $\gamma$ -ray MSPs. This upper limit is a strict constraint on the  $\gamma$ -ray emission of IGR J00291+5934, which likely suggests that this source may not emit in  $\gamma$ -ray band, or its  $\gamma$ -ray beam, at least the bright portion of its  $\gamma$ -ray beam, may not cross the earth. For SAX J1808.4–3658, its  $\gamma$ -ray conversion efficiency is  $< 57\%$ , which is not sufficiently low suggesting this source as a candidate  $\gamma$ -ray source for further monitoring with longer observation time.

It can be noted that PSR J1023+0038 has been detected with the lowest conversion efficiency of  $\sim 0.5\%$  in  $> 100$  MeV band (Figure 2; derived from spectral parameters given in Tam et al. 2010). This may suggest

that  $\gamma$ -ray emission of MSPs are related to their evolutionary stage. The fast rotating AMPs may have almost no  $\gamma$ -ray emission, but at the end of the accreting phase the newly born MSPs begin to emit in  $\gamma$ -ray band with low  $\gamma$ -ray conversion efficiencies. We have also searched for pulsed emission from J1023+0038 in the *Fermi* data from 2008 to the present time (data in Tam et al. 2010 were to 2010 July), but with no detection. Comparisons of the properties of its  $\gamma$ -ray pulsed emission with that of its radio emission may have implications to what are expected from AMPs. On the other hand, we note that a possible ‘death line’,  $\eta_\gamma = 10^{0.32\tau_9 - 4.3}$  where  $\tau_9$  is the characteristic age in units of  $10^9$  yrs, may exist in Figure 2, below which no  $\gamma$ -ray MSPs have been detected. If this is true, SAX J1808.4–3658 would have no  $\gamma$ -ray emission because its conversion efficiency upper limit is very close to this death line. Hopefully with more MSPs detected by *Fermi* in the near future, whether this death line exists or not can be verified.

It is worth pointing out that our evaluations of the upper limits on  $\gamma$ -ray emission from the four AMPs have a few uncertainties, which include that from the LAT instrument response function, Galactic diffuse emission, and nearby sources' emission. Data of longer monitoring by *Fermi*/LAT will help reduce the uncertainties and thus provide tighter constraints on the emission properties of the AMPs.

This research was supported by the starting funds of Shanghai Astronomical Observatory, National Basic Research Program of China (973 Project 2009CB824800), and National Natural Science Foundation of China (11073042). ZW is a Research Fellow of the One-Hundred-Talents project of Chinese Academy of Sciences.

## REFERENCES

- Abdo, A. A., Ackermann, M., Ajello, M., et al. 2009, *Science*, 325, 848  
—, 2010a, *ApJ*, 712, 957  
—, 2010b, *ApJS*, 188, 405  
—, 2010c, *ApJS*, 187, 460  
Alpar, M. A., Cheng, A. F., Ruderman, M. A., & Shaham, J. 1982, *Nature*, 300, 728  
Archibald, A. M., et al. 2009, *Science*, 324, 1411  
Atwood, W. B., Abdo, A. A., Ackermann, M., et al. 2009, *ApJ*, 697, 1071  
Bhattacharya, D., & van den Heuvel, E. P. J. 1991, *Phys. Rep.*, 203, 1  
Burderi, L., Di Salvo, T., D’Antona, F., Robba, N. R., & Testa, V. 2003, *A&A*, 404, L43  
Burgay, M., et al. 2003, *ApJ*, 589, 902  
Campana, S., et al. 2004, *ApJ*, 614, L49  
Chakrabarty, D., & Morgan, E. H. 1998, *Nature*, 394, 346  
Cheng, K. S., Ho, C., & Ruderman, M. 1986, *ApJ*, 300, 500  
Cognard, I., Guillemot, L., Johnson, T. J., et al. 2011, *ApJ*, 732, 47  
D’Avanzo, P., Campana, S., Casares, J., et al. 2009, *A&A*, 508, 297  
D’Avanzo, P., Campana, S., Covino, S., et al. 2007, *A&A*, 472, 881  
Deloye, C. J., Heinke, C. O., Taam, R. E., & Jonker, P. G. 2008, *MNRAS*, 391, 1619  
Falanga, M., Kuiper, L., Poutanen, J., et al. 2005, *A&A*, 444, 15  
Freire, P. C. C., Abdo, A. A., Ajello, M., et al. 2011, *Science*, 334, 1107  
Galloway, D. K. 2006, in *American Institute of Physics Conference Series*, Vol. 840, *The Transient Milky Way: A Perspective for MIRAX*, ed. F. D’Amico, J. Braga, & R. E. Rothschild, 50–54  
Galloway, D. K., Chakrabarty, D., Morgan, E. H., & Remillard, R. A. 2002, *ApJ*, 576, L137  
Guillemot, L., Freire, P. C. C., Cognard, I., et al. 2012a, *MNRAS*, 422, 1294  
Guillemot, L., Johnson, T. J., Venter, C., et al. 2012b, *ApJ*, 744, 33  
Hartman, J. M., Patruno, A., Chakrabarty, D., et al. 2009, *ApJ*, 702, 1673  
Homer, L., Charles, P. A., Chakrabarty, D., & van Zyl, L. 2001, *MNRAS*, 325, 1471  
Iacolina, M. N., Burgay, M., Burderi, L., Possenti, A., & di Salvo, T. 2009, *A&A*, 497, 445  
in ’t Zand, J. J. M., Heise, J., Muller, J. M., et al. 1998, *A&A*, 331, L25  
Jonker, P. G., Torres, M. A. P., & Steeghs, D. 2008, *ApJ*, 680, 615  
Keith, M. J., Johnston, S., Ray, P. S., et al. 2011, *MNRAS*, 414, 1292  
Kerr, M., Camilo, F., Johnson, T. J., et al. 2012, *ApJ*, 748, L2  
Larsson, S. 1996, *A&AS*, 117, 197  
Muslimov, A. G., & Harding, A. K. 2004, *ApJ*, 606, 1143  
Pallanca, C., Mignani, R. P., Dalessandro, E., et al. 2012, *ApJ*, 755, 180  
Papitto, A., di Salvo, T., Burderi, L., et al. 2007, *MNRAS*, 375, 971  
Patruno, A. 2010, *ApJ*, 722, 909  
Patruno, A., Bult, P., Gopakumar, A., et al. 2012, *ApJ*, 746, L27  
Patruno, A., & Watts, A. L. 2012, *ArXiv e-prints*

- Ransom, S. M., Ray, P. S., Camilo, F., et al. 2011, *ApJ*, 727, L16
- Ruderman, M. A., & Sutherland, P. G. 1975, *ApJ*, 196, 51
- Srinivasan, G. 2010, *New A Rev*, 54, 93
- Strohmayer, T. E., Markwardt, C. B., Swank, J. H., & in't Zand, J. 2003, *ApJ*, 596, L67
- Takata, J., Cheng, K. S., & Taam, R. E. 2012, *ApJ*, 745, 100
- Tam, P. H. T., Hui, C. Y., Huang, R. H. H., et al. 2010, *ApJ*, 724, L207
- van Paradijs, J., & McClintock, J. E. 1995, *Optical and Ultraviolet Observations of X-ray Binaries (X-ray Binaries, eds. W.H.G. Lewin, J. van Paradijs, and E.P.J. van den Heuvel, Cambridge: Cambridge Univ. Press)*, 58
- Wang, X., Wang, Z., & Morrell, N. 2012, *ArXiv e-prints*
- Wang, Z., Archibald, A. M., Thorstensen, J. R., et al. 2009a, *ApJ*, 703, 2017
- Wang, Z., Bassa, C., Cumming, A., & Kaspi, V. M. 2009b, *ApJ*, 694, 1115
- Wijnands, R., & van der Klis, M. 1998, *Nature*, 394, 344

TABLE 1  
OBSERVATIONAL PROPERTIES OF THE FOUR AMP TARGETS

Source name	$d$ (kpc)	$\nu$ (Hz)	$\dot{\nu}$ ( $10^{-15}$ Hz s $^{-1}$ )	$E_{sd}$ ( $10^{33}$ ergs s $^{-1}$ )	$\tau$ ( $10^9$ yrs)	$L_\gamma$ ( $10^{33}$ ergs s $^{-1}$ )	$\eta_\gamma$
SAX J1808.4–3658	3.5 <sup>a</sup>	400.97521024 <sup>f</sup>	-0.55 <sup>f</sup>	9	11.56	<5.1	<0.57
IGR J00291+5934	5 <sup>b</sup>	598.89213061 <sup>g</sup>	-3.0 <sup>g</sup>	70	3.17	<2.1	<0.03
XTE J1814–338	8 <sup>c</sup>	314.35610879 <sup>h</sup>	–	–	–	<12	–
XTE J0929–314	6 <sup>d,e</sup>	185.105259 <sup>i</sup>	–	–	–	<2.2	–

NOTE. — Column 5 are the spin-down luminosities of the sources with spin-down rate measurements. Column 6 lists the characteristic ages derived by  $\nu/2\dot{\nu}$ . Column 7 lists the 100 MeV to 300 GeV  $\gamma$ -ray luminosity upper limits resulting from binned likelihood analysis of the LAT data with  $\Gamma$  and  $E_{cut}$  of the spectral models of these sources fixed to 1.4 and 1.6 GeV. Column 8 are the 100 MeV to 300 GeV  $\gamma$ -ray conversion efficiency upper limits for the sources with measurements of spin-down rates. a: Galloway 2006. b: Falanga et al. 2005. c: Strohmayer et al. 2003. d: Galloway et al. 2002. e: Iacolina et al. 2009. f: Time of ascending node is MJD 52499.9602472 (Hartman et al. 2009). g: Time of ascending node is MJD 54692.0 (Patruno 2010). h: The epoch time is MJD 52797.27387859868 (Papitto et al. 2007). i: The epoch time is MJD 52405.48676 (Iacolina et al. 2009).

TABLE 2  
OBSERVATIONAL PROPERTIES OF THE 20 CONFIRMED  $\gamma$ -RAY MSPs IN THE *Fermi* 2-YEAR CATALOG.

Source Name	$d$ (kpc)	$\nu$ (Hz)	$\dot{\nu}$ ( $10^{-15}$ Hz s $^{-1}$ )	$E_{sd}$ ( $10^{33}$ ergs s $^{-1}$ )	$\tau$ ( $10^9$ yrs)	$L_\gamma$ ( $10^{33}$ ergs s $^{-1}$ )	$\eta_\gamma$
J0030+0451*	0.3 <sup>a</sup>	205.3 <sup>b</sup>	-0.4 <sup>b</sup>	3	7.72	$0.67 \pm 0.02$	$0.197 \pm 0.007$
J0034–0534	0.5 <sup>c</sup>	531.9 <sup>c</sup>	-1.4 <sup>c</sup>	30	5.96	$0.55 \pm 0.05$	$0.018 \pm 0.002$
J0101–6422	0.6 <sup>d</sup>	389.1 <sup>d</sup>	-0.8 <sup>d</sup>	12	7.84	$0.39 \pm 0.04$	$0.032 \pm 0.004$
J0218+4232*	2.7 <sup>a</sup>	431.0 <sup>b</sup>	-14.3 <sup>b</sup>	243	0.48	$41 \pm 2$	$0.17 \pm 0.01$
J0437–4715*	0.2 <sup>a</sup>	173.6 <sup>b</sup>	-0.4 <sup>b</sup>	3	6.52	$0.054 \pm 0.004$	$0.018 \pm 0.001$
J0610–2100	3.5 <sup>e</sup>	263.2 <sup>e</sup>	-0.9 <sup>e</sup>	9	4.88	$12 \pm 2$	$1.3 \pm 0.3$
J0613–0200*	0.5 <sup>a</sup>	326.8 <sup>b</sup>	-1.0 <sup>b</sup>	12	5.39	$0.85 \pm 0.06$	$0.068 \pm 0.005$
J0614–3329	1.9 <sup>f</sup>	317.5 <sup>f</sup>	-1.8 <sup>f</sup>	22	2.85	$48 \pm 1$	$2.2 \pm 0.1$
J0751+1807*	0.6 <sup>a</sup>	287.4 <sup>b</sup>	-0.5 <sup>b</sup>	6	9.20	$0.67 \pm 0.07$	$0.12 \pm 0.01$
J1231–1411	0.4 <sup>f</sup>	271.7 <sup>f</sup>	-1.7 <sup>f</sup>	18	2.56	$2.02 \pm 0.06$	$0.112 \pm 0.003$
J1614–2230*	1.3 <sup>a</sup>	317.5 <sup>b</sup>	-0.4 <sup>b</sup>	5	12.49	$4.6 \pm 0.4$	$0.91 \pm 0.08$
J1744–1134*	0.5 <sup>a</sup>	245.7 <sup>b</sup>	-0.4 <sup>b</sup>	4	9.22	$0.94 \pm 0.07$	$0.23 \pm 0.02$
J1823–3021A	8.4 <sup>g</sup>	183.8 <sup>g</sup>	-114.2 <sup>g</sup>	829	0.03	$133 \pm 23$	$0.16 \pm 0.03$
J1959+2048	2.5 <sup>h</sup>	625.0 <sup>h</sup>	-6.6 <sup>h</sup>	163	1.50	$12 \pm 1$	$0.077 \pm 0.009$
J2017+0603	1.6 <sup>i</sup>	344.8 <sup>i</sup>	-1.0 <sup>i</sup>	13	5.54	$11.0 \pm 0.7$	$0.82 \pm 0.05$
J2043+1710	1.8 <sup>j</sup>	420.2 <sup>j</sup>	-0.9 <sup>j</sup>	15	7.20	$11.4 \pm 0.8$	$0.74 \pm 0.05$
J2124–3358*	0.3 <sup>a</sup>	202.8 <sup>b</sup>	-0.5 <sup>b</sup>	4	6.51	$0.28 \pm 0.01$	$0.070 \pm 0.004$
J2214+3000	1.5 <sup>f</sup>	320.5 <sup>f</sup>	-1.4 <sup>f</sup>	18	3.53	$8.9 \pm 0.5$	$0.49 \pm 0.03$
J2241–5236	0.5 <sup>k</sup>	457.3 <sup>k</sup>	-1.4 <sup>k</sup>	25	5.19	$1.02 \pm 0.06$	$0.042 \pm 0.002$
J2302+4442	1.2 <sup>i</sup>	192.7 <sup>i</sup>	-0.5 <sup>i</sup>	4	6.19	$6.7 \pm 0.4$	$1.8 \pm 0.1$

NOTE. — Observational properties of the 20 confirmed  $\gamma$ -ray MSPs in *Fermi* 2-year catalog. The sources marked with \* are the first eight  $\gamma$ -ray MSPs detected by *Fermi*/LAT. Column 2 lists the distance of each source. Columns 3 and 4 list the frequency and spin-down rate of each source. Column 5 lists the spin-down luminosities of sources. Column 6 lists the characteristic ages derived by  $\nu/2\dot{\nu}$ . Column 7 lists the 100 MeV – 100 GeV  $\gamma$ -ray luminosities derived from catalog. Column 8 lists the 100 MeV – 100 GeV  $\gamma$ -ray conversion efficiencies. The uncertainties of luminosities and efficiencies are derived from flux uncertainties, the distance uncertainties are not considered here. a: Abdo et al. 2009. b: Abdo et al. 2010c. c: Abdo et al. 2010a. d: Kerr et al. 2012. e: Pallanca et al. 2012. f: Ransom et al. 2011. g: Freire et al. 2011. h: Guillemot et al. 2012b. i: Cognard et al. 2011. j: Guillemot et al. 2012a. k: Keith et al. 2011.

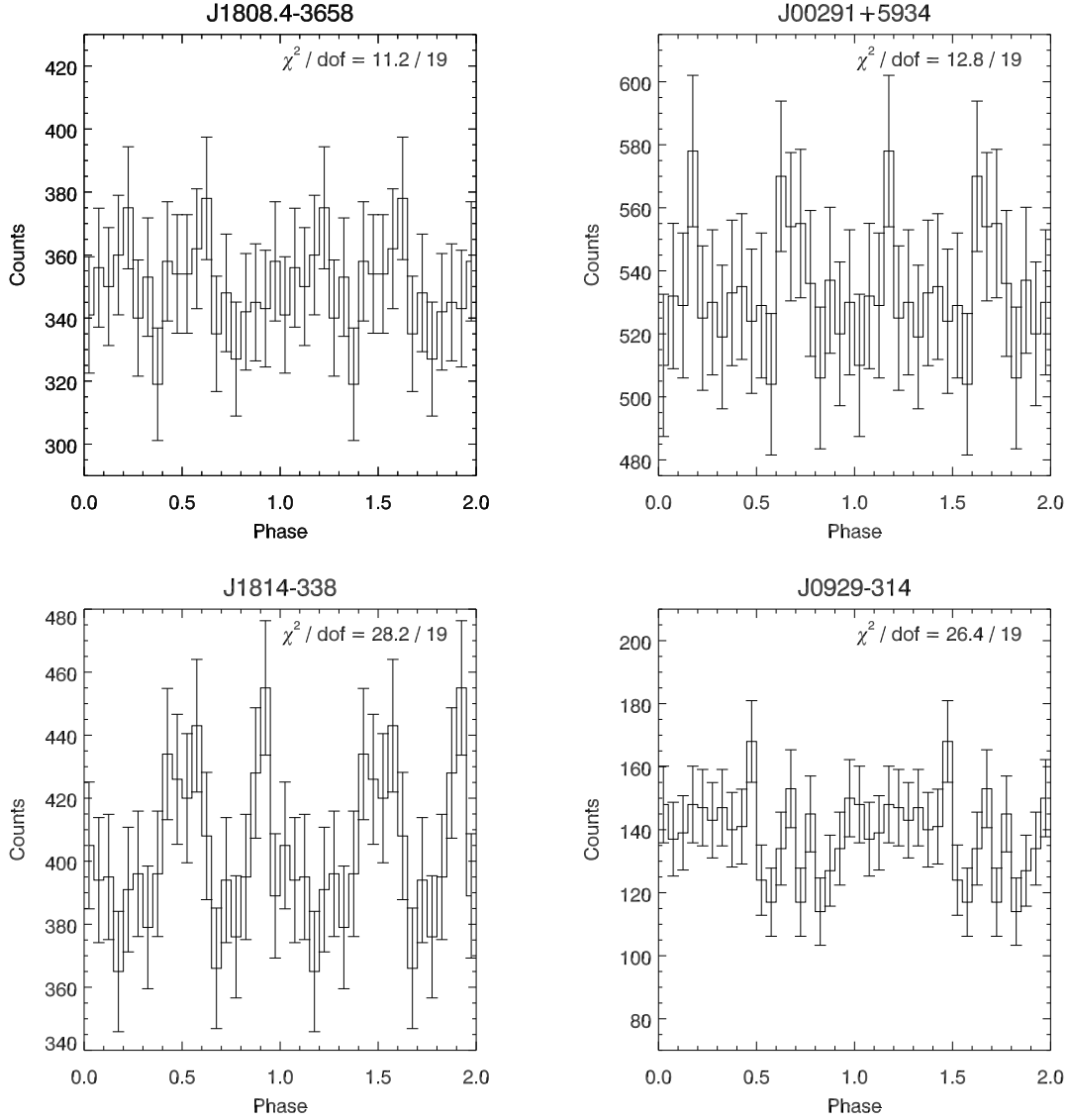


FIG. 1.— 100 MeV – 300 GeV folded light curves of the four AMPs included in our work. The phase resolution of each light curve is 0.05. The spin parameters we used in epoch folding are those listed in Table 1. For each light curve we made the  $\chi^2$  test and the obtained  $\chi^2/\text{dof}$  values are given in the upper right corner of each panel.

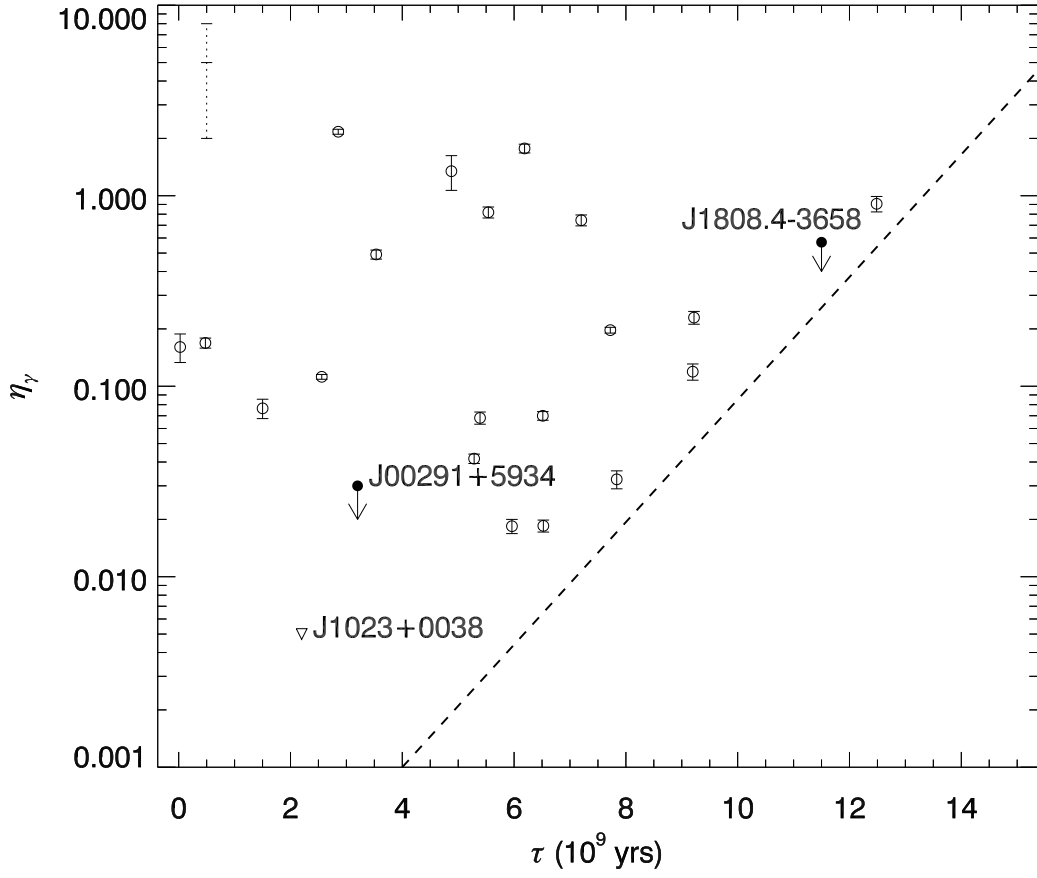


FIG. 2.—  $\gamma$ -ray conversion efficiencies and characteristic ages of MSPs, with our two AMP targets included. The open circles represent the confirmed MSPs in the *Fermi* 2-year catalog, and the filled circles with arrows represent SAX J1808.4–3658 and IGR J00291+5934. The open triangle represents the newly born MSP PSR J1023+0038. The errors of data points are derived from flux uncertainties. The dotted bar in the top left of the figure represents errors derived from distance uncertainties which are assumed to be 30% of the distance values. The dashed line indicates a possible ‘death line’,  $\eta_\gamma \sim 10^{0.32\tau_9 - 4.3}$ .